Non-Destructive Assessment of Living Trees by using Electric Resistive Tomography

ZOLTAN VIZVARI[1], ATTILA TOTH[2], FERENC DIVOS[3], MIHALY KLINCSIK[4], ZOLTAN SARI[5], PETER ODRY[6]
[1]Department of Environmental Engineering, Faculty of Engineering and Information Technology, University of Pécs, Pécs, HUNGARY
[2]Institute of Physiology, Medical School, University of Pécs, Pécs, HUNGARY
[3]Doctoral School on Materials Sciences and Technologies, Óbuda University, Budapest, HUNGARY
[4]Department of Mathematics, Faculty of Engineering and Information Technology, University of Pécs, Pécs, HUNGARY
[5]Department of Information Technology, Faculty of Engineering and Information Technology, University of Pécs, Pécs, HUNGARY
[6]Institute of Information Technology, University of Dunaujvaros, Dunaújváros, HUNGARY
[1]vizvari.zoltan@mik.pte.hu, [2]attila.toth@aok.pte.hu, [3]divos@fakopp.com, [4]klincsik@mik.pte.hu, [5]sari.zoltan@mik.pte.hu, [6]podry@uniduna.hu

Abstract: - Electric Resistive Tomography is one of the latest procedures in the assessment of living trees. There is a growing interest regarding this measurement method yet despite the presence of such measuring devices on the market, this method, unlike acoustic assessment techniques for trees, is far from being fully developed. The devices available on the market analyze only the nature of resistivity of the device, but do not take into account the phase character of the measurements. In addition to measurement information, this paper presents several results regarding fixed impedance tomography. The experience gained here is to be used for further research.

Key-Words: - non-destructive assessment of materials, assessment of living trees, Electrical Impedance Tomography

1 Introduction

The importance of non-destructive assessment techniques in the case of living trees is unquestionable. In regards to both technical and biological reasons, special emphasis is placed on assessing the condition of living trees, which is also important in the areas of forest management and wood-based industries. In consideration of the available measurement procedures, non-destructive or non-invasive methods are particularly significant [1]. A group of non-destructive measurement techniques, geophysical measurements, should be given high priority, since the conditions of the measurements are highly similar to the research area of the present paper. In both cases, the objective is to map a particular structure (geological formation, or, in the present case, a tree trunk) in as much detail as possible and as much as the circumstances allow, without penetrating the sensor inside the structure, i.e., without damaging the structure [6]. Thus, these measurements can be made with transmitters and receivers positioned along the circumference of the assessed structure, while the receivers record the changes in the exciting signal emitted by the transmitter.

Acoustic-seismic research methods, the branch of geophysical metrology practice which is the most widespread and has the most extensive published literature, has been adopted for assessing living trees for many years. This method is widely used in non-invasive assessment of living trees by mapping the tree structure based on its density, since it affects the velocity of the acoustic wave passing through the tree. This fact, however, also depicts the limitations of this method, as it can only detect the significant changes in density (i.e., physical changes) inside the tree (cavities, decay, etc.) [7] – [11].

If one also wishes to obtain data regarding the chemical changes inside the assessed structure, another geophysical measurement procedure has to be applied: geo-electrical/electromagnetic measurements for assessing living trees [4]. The name of the method is Electrical Impedance Tomography (henceforth EIT). EIT creates an impedance map of the tree structure which can be used for making deductions in reference to the distribution of moisture, cell structure, and electrolyte content distribution inside the structure [Acta Silvatica]. EIT is a measurement technique which is still under development in the case of tree structures, and its biggest obstacle is the low spatial resolution of the measurements. Despite this, there are impedance tomography devices available on the market, one of them being PICUS Treetronic [1] – [5], which has also been used in the present research. However, the aim here is to introduce a new device interface (already being tested in biomedical procedures at the University of Pécs) and to develop a new mathematical backbone to this interface (already in progress).

In the present paper, in addition to the physical fundamentals of EIT, the geo-electrical measurement procedure adopted for assessing living trees is also briefly summarized. In the following sections, the measuring device and some measurements made with it are described in detail.

The instruments available on the market generate ERT (Electric Resistive Tomography) results (such as [16]). ERT does not take into account the phase character of dielectrics, thus providing a limited view of the dielectric structure of the assessed material. However, according to the results of chemical spectroscopy, the phase character of dielectrics also plays a role in assessing the structure of materials. The current research is aimed at developing an EIT device capable of measuring impedance including the introduction of this measurement procedure into the practice of assessing living trees with results in an impedance tomographical method which provides an evaluation and is of a higher resolution than when compared to that of the the current methods.

2 The Physical Fundamentals of EIT

In the case of EIT, an electric field is generated in the structure of the assessed object, after which its complex electrical conductivity can be deduced by measuring certain parameters (e.g., the potential difference) and detecting the distortion of the electric field. The physical background of the measurements is based on the system of the Maxwell equations used for describing electrodynamic phenomena [12]. In the case of EIT, excitation occurs with a sinusoidal alternating current, and consequently the Maxwell equations are considerably simplified, since the introduction of temporally constant currents results in the following equations [12]:

$$\nabla \times \mathbf{H} = \mathbf{J} \tag{1}$$

$$\nabla \times \mathbf{E} = 0 \tag{2}$$

$$\nabla \cdot \mathbf{B} = 0 \tag{3}$$

$$\nabla \cdot \mathbf{D} = \rho \tag{4}$$

As EIT measurements are principally made at low frequencies (the maximum frequency in the current research is 100 kHz), the magnetic phenomena occurring during the measurements are negligible [13]; thus, equations (2) and (4) count as the basic equations of the EIT measurements. Following the systematizing of the equations, the partial differential equation used as a starting point for the EIT measurements is [13]:

$$\nabla \cdot \sigma \nabla \phi = 0 \tag{5}$$

which can be solved by specifying the commonly referred to Dirichlet or Neumann boundary conditions, or both of them simultaneously. There are several mathematical methods available regarding the solution. One is the Finite Element Method (FEM, [13]), another is the Boundary Element Method (BEM, [14]), yet another is the method of Finite Differences (FD) etc.

The aim during the measurements is to restore the location-dependent conductivity σ in equation (5). Various inverse problem-solving methods are available for this task [15]:

- linear methods: LBP, linear back projection,
- non-linear methods, and
- heuristic (empirical) methods.

With respect to measuring geometry, EIT measurements can be divided into two main groups:

1. if the electrodes are placed on the ground, the particular geometry can be modeled with an infinite half-space;
2. if the sensors are placed on a living tree in a circular shape, the measurements can be modeled as a closed manifold.

EIT measurements on living trees rely on the principle of surface geo-electric measurements. EIT measures apparent specific resistance. The determination of the apparent specific resistance is the simplest in geo-physical measurements when the sub-soil is made up of rocks which have identical specific resistance in all directions, i.e., when it can be replaced with a homogenous half space. On the surface of the homogenous half space (Fig. 1.), in points A and B, current IAB is excited with a generator during the measurements. If the resulting voltage ΔVMN of excitation generated between points M and N is measured, then the apparent specific resistance of the rock can be expressed as [6]:

$$\rho_L = K \frac{\Delta V_{MN}}{I_{AB}} \qquad (6)$$

Amount K in the equation is the often referred to configurational coefficient. The measurement layout is illustrated in Fig. 1., which illustrates the electric field of the AMNB (Schlumberger) electrode array:

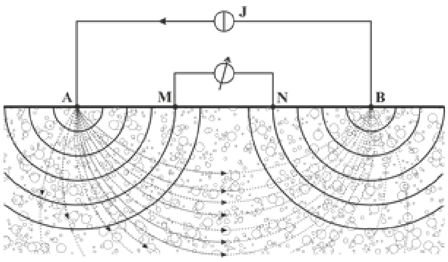

Fig. 1: The arrangement of the electrodes, an image of the current lines and surface potentials in homogenous, isotropic sub-soil with an AMNB, Schlumberger array [6]

During the measurements, the supplied current has a known value IAB. The dotted line represents the current space of the two power electrodes which can be modeled as point sources, whereas the full lines depict the equipotential surfaces of the generated current space, the potential difference between which can be measured with electrodes M and N (ΔVMN).

The penetration of the generated current space at the midpoint of the power electrodes is approximately five times their distance, since 90% of the total current is concentrated in this volume. [6] Consequently, both the current density and the current flow rate remain constant, if the penetration is kept constant. In the first approximation, the penetration of the current is proportional to the distance of the power electrodes, if this result is extrapolated to the inhomogeneous half space.

Manual evaluation and illustration methods prior to the 1990s have been replaced by computerized evaluation techniques, due to the rapid development of mathematical modeling. Improved 2D and 3D electrical sectioning methods have been introduced to determine the resistance distribution of a flat section in case of 2D, or to define the resistance profile of a space section by using several dozens of electrodes in case of 3D. Therefore, the results of the measurements are practically obtained in a particular space, both by sectioning and by probing.

Such a form in matching 2D measuring method was used in assessing living trees as well, whereby during EIT measurements, a modified variant of the axial dipole measurement arrangement widely used in geo-physical practice was applied. The first independent measurement procedure used for assessing living trees was described in a paper published in [21].

3 The Applied Measuring Device and Measurement Method

In the current research, the measurements were made using a PICUS Treetronic EIT device manufactured by the German Argus Electronic GmbH. Instead of determining the impedance, this measuring instrument only deals with the resistance value, and since it neglects the phase character of impedance, the result of its measurement is ERT (Electric Resistive Tomography). In the current research, an impedance tomography device is being developed.

The major parts of the measuring device are (Fig. 2.):

- numbered measuring cables, which are responsible for connections in the appropriate order between the electrodes and the measuring system,
- an AD converter and multiplexer unit, the role of which is to connect the generator and the measuring channels to the electrodes corresponding to the measuring algorithm, and to digitize the measured analog signal,
- the measuring unit processes the measured signals and forwards them via Bluetooth to the measuring software installed on a PC, which performs data collection and measurement evaluation.

Fig. 2: The PICUS Treetronic measuring system [16]

The number of electrodes, i.e., the number of channels used is determined by the purpose of the measurement. For example, to detect false heartwood, it is sufficient to make the measurement using fewer channels, whereas for measuring other, more detailed structures, it is advisable to increase the number of channels to obtain effective results. This, however, significantly increases the time taken to perform the measurement. Fig. 3. shows a test-arrangement ready to be used:

Fig. 3: Installing electrodes to a tree trunk at chest level

The ADC and the multiplexer unit were located under electrode no. 1. Instead of electrodes, simple nails were used and were connected to the appropriately numbered cables via alligator clips. The PICUS Treetronic tomograph can be used for performing measurements only with one type of impedance tomography electrode configuration. This is the arrangement known in geo-physical measurements as a dipole axial arrangement. Fig. 4. also shows how the PICUS Treetronic also uses the notations A and B traditionally accepted in geo-physical research for the position of the generator, and M and N for the measuring channels. The principle of the measuring method is illustrated below, in Fig. 4:

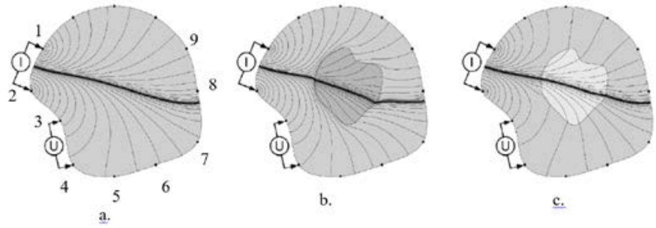

Fig. 4: The principle of EIT in assessing living trees (a. homogenous distribution of conductivity b. and c. examples for inhomogeneous distribution of conductivity) [16]

The measuring device connects the generator (exciting signal) and simultaneously the measuring channel to a pair of electrodes. In this case, excitation is always triggered, and measurements are always performed on adjacent electrodes (Fig. 4.). During the measurement, the device registers the current flowing through the system and the measureable potential difference between electrodes M and N. In addition to the configuration, Fig. 4. also shows the electric field generated within the measured range. If the assessed area is assumed to be homogenous, isotropic (Fig. 4.a.) and electrically conductive (and the area outside the assessed area is assumed to be an insulator), the supplied electric current fills the entire area, or, according to charge retention, it flows between the terminals of the current generator (marked with I in Fig. 4.). Fig. 4. shows the isopotential lines of the potential field generated by the current space, which are formed in accordance with the current density between the terminals of the current generator: in the vicinity of the electrodes, due to a higher current density, the isopotential lines are closer to one another, whereas the more distant they are from the electrodes, the more they become sparse and straightened, and become denser again along the thick line. The potential field in Figures 4.b. and 4.c. is noticeably asymmetric, since the inhomogeneity of the conductivity distorts it. During the measurements, the distances A-B and M-N were constant; however, the distance between the pairs of electrodes (distance B-M) varied. The length of the data collection series depends on the number of electrodes; therefore, its maximum value n is half of the total number of electrodes. Prior to starting the measurement, it is possible to interfere with the measurement process on some level; however, this is essentially completely automatic. When utilizing the maximum number of channels, i.e., measurements with 24 electrodes, the measurement system registers 252 data packets. For each data packet, 4 parameters are recorded:

– I+ the current flowing through the system and U+ the voltage measured on electrodes M and N (potential difference),
– I- the current flowing through the system after the polarity switch of the generator and U- the voltage measured on electrodes M and N (potential difference).

During the measurement, the amplitude of the generator is automatically regulated by a servo system, to avoid exiting the measuring range. The software informs the detector about this. Once the measurement has been completed, data is saved separately, and the tomogram can be created in support of the evaluation.

4 EIT Measurements Performed on Living Trees

The measurements were made in an oak forest in the municipality of Darány (County Somogy) with the PICUS Treetronic ERT device. The subject of the analysis was two tree species:

1. A population of middle-aged Austrian oak (quercus cerris), and
2. an adjacent population of old common oak (quercus robur).

Typically, the soil of the area is the same sour sandy soil characteristic of the inner parts synonymous with Somogy County. Three specimens of Austrian oak which seemed to be healthy after visual inspection were selected from the Austrian oak population located in this area. 6 electrodes were placed at chest level onto them and the EIT measurements were performed. The measurement results are shown in Fig. 5:

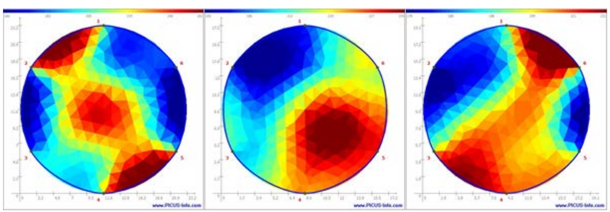

a b c

Fig. 5: The EIT measurement results performed on middle-aged Austrian oaks (Ωm)

Fig. 5 illustrates the appropriate measurement results of three specimens. The purpose of the assessment regarding this measurement series was to familiarize the users with the operational functionality of the device and the resulting tomograms once a relatively low number of electrodes had been implemented. In all three measurements, 6 electrodes were used to create the tomogram, which resulted in a total of 36 measured values per trunk. These were used to create the diagrams shown in Figure 5.1. Due to its high resistance, the tree bark can be considered an insulator, and the current could not penetrate it; therefore, the nails used as electrodes had to penetrate through the bark (cambium), which is is why the effect of the bark cannot be seen in the resulting tomogram. Thus, the tomographical images shown in Figure 5.1. practically approximate the distribution of resistance of the sapwood and the heartwood. First, a 73 cm-diameter Austrian oak was selected. In Fig. 5.a, it is relatively distinguishable, since the resistance of the heartwood (the flat area around the center of the circle) is higher than when compared to most of the sapwood surrounding it. It is also noticeable in which the center has a maximum value of resistance, which gradually decreases toward the exterior. Based on the resistance image, the resistance-distribution of the sapwood can be divided into two parts. On the one hand, the sapwood consists of two diametrically opposed parts of higher resistance (between electrodes 1 and 2, including the area between electrodes 4 and 5), which contain the maximum values regarding the tomogram; on the other hand, it also consists of two diametrically opposed blue bands, which, however, refers to the part of the image with the minimal specific resistance. The color range of Fig. 5.a is linear, with a minimum of 166 Ωm and a maximum of 261 Ωm, therefore, encompassing a range of specific resistance of ca. 100 Ωm. Fig. 5.b. was obtained from a 54 cm-diameter Austrian oak, highlights a completely different distribution. The resistance distribution shown in Fig. 5.a is typical of the sapwood and is not visible here. The tomogram shows two distinctly separated zones. The minimum resistance values can be seen between electrodes 1 and 2, whereas the maximum values are surrounding electrode 5. In the observation of the color range, it is noticeable when compared to the previous image, the resistance range has decreased considerably, since the colors are distributed between 200 – 234 Ωm. Consequently, if the limits of resistance of Fig. 5.a were to be set here as well, the contrast of the image would decrease to such a degree in which the currently visible variations will be less pronounced. Finally, an Austrian oak with a 60 cm-radius was analyzed. In Fig. 5.c (compared to Fig. 5.a), the granularity of the sapwood is visible. Here, the parts with high resistance are around electrodes 1 and 6, including at or in the vicinity of 4 and 3, while the parts with low resistance are around electrode 2 and between electrodes 5 and 6. In this image, the resistance of the heartwood is not so pronounced as in Fig. 5.a, however, it is visible in which the area around the center has higher resistance. The color range is linear in this case, too, with a minimum of 178 Ωm and a maximum of 232 Ωm.

Following the measurements taken with a low number of electrodes, it was determined to increase the number of electrodes, i.e., the number of the measuring channels, to be able to study the measuring process. To this end, three common oaks were selected, and EIT measurements were made with electrodes also positioned at chest level. Accordingly, the EIT sections of the measurements performed on the three common oaks are shown in Fig. 6:

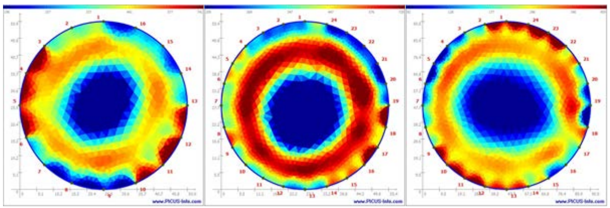

a b c

Fig. 6: EIT tomograms of measurements performed on old common oaks (Ωm)

In case of the measurement with 16 channels, the tomograms were created from 416 numerical values, while in case of the 24-electrode measurements, 1008 numerical values were used for the tomograms. Fig. 6. shows that when compared to the middle-aged Austrian oaks, here, the device creates a completely different pattern, which is generally characterized by a distinctly prominent ring with higher resistance than what is measured in the center. It is also noticeable in all three images in which the circular area around the center is the minimum of the tomogram, and therefore, it is clearly distinct from the ring with higher resistance surrounding it. By a more careful examination, it can also be observed in which the low-high divided edge shown in Fig. 5. is present here as well, with the same 90°-alternation. If the resistance images are to be examined separately, it can be concluded how Figures 6.a and 6.b are essentially, very similar, one to the other. The resistance scale is linear with a minimum of 200 Ωm and a maximum of ca. 730 Ωm. The geometrical dimensions of the trees were roughly identical (in case of Fig. 6.a, the circumference of the trunk was 160 cm, while in Fig. 6.b, it was 174 cm), which supports the similarity. In Fig. 6.c, the circumference (300 cm) was almost double of the previous two. Essentialy, this implies the tree is also older. If the results of the EIT measurements performed on it are closely examined, there are no visible changes, yet, if the boundaries of the color range (92 – 459 Ωm) are inspected, it can be noticed in absolute terms, the resistance of the section has decreased. In addition, it can also be seen in which the difference between the central part with the low resistance and the maximum of the ring with the higher resistance has decreased compared to the other two images.

The results of the measurements regarding the two tree species are different in nature, however, the granularity of the sapwood is a common feature in all the showcased patterns.

5 Conclusion

In the present paper, a relatively new and currently still not fully developed technique of non-destructive assessment of living trees has been presented, starting from its physical fundamentals. Since it is an adaptation of a routinely implemented geo-physical procedure, it was necessary to provide a general introduction of the starting method of EIT in surface geo-electric arrays. Of course, the analogy of what has been described there can also be found in the sections describing the measuring device and the measurement method. Afterward, the measurement results obtained in the current research have been presented with the aim of a deeper understanding of the measuring device.

Distinctly, the purpose of the current research is developing EIT measurements for simulated and real measurement procedures, introducing a new, multi-channel, high-resolution measuring device into the methodology of EIT tree assessment, and developing a tomographical measuring method and evaluation for trees. Additionally, it was considered important to gain a comprehensive understanding of an EIT device, currently available on the market, which can be used as a reference point in the subsequent research tasks. This is why the PICUS

Treetronic EIT measuring device manufactured by Argus Electronic GmbH was chosen.

The operation of the measuring device can be understood with the help of geo-physical fundamentals. Even the placement of the electrodes is the same as in geo-physical practice. However, when assessing trees and performing a high number of measurements, this often results in making the process very time-consuming. The measurement method is practically identical with geo-electric tomography which today, is widespread in geo-physics. Unfortunately, an EIT measurement can only be made with the device in the dipole axial arrangement. Another disadvantage of inflexibility is, in many cases, the applied method does not suit appropriately the purpose of the measurement. However, its great advantage is in the measuring algorithm, which can be programmed far more easily and is consequently easier to implement. The data collected during the measurements can only be analyzed in the PICUS measurement software, no temporary file is created with the data, and they cannot be extracted.

The imaging algorithm is based on the Finite Element Method (FEM). This can be seen in Figures 5. and 6. as well, in which it is clearly visible the measuring range is divided into triangles which the software fills in with a certain hue, thus assuming a homogenous specific resistance within a single triangle. The result of the calculation is the distribution of specific resistance along the plane of a particular range. The tomograms are in color and the color range is indicated on a linear scale by the software. The evaluation, i.e., the imaging is done off-line, which means the collected data make up practically the saved information, and thus the calculation has to be reaccomplished folllowing each time data is loaded. This way, of course, the calculations can be done with various parameters, however, it slows down the on-site evaluation.

These findings are very important regarding the instrument and its method currently undgoing development in areas of research, as, according to future plans, they will contribute to correcting the above shortcomings. The measurements will be performed on multiple channels, in parallel. This has the advantage which technically, the 252 measurements imply 252 switches in support of the measuring device, whereas by measuring on multiple, for example 8 channels, one excitation position can be covered during a single measurement, and thus, the measurement can be accelerated and the sensitive points during the measurements, i.e., the number of connections can be reduced.

In terms of evaluation and the imaging algorithm, the Finite Element Method is to be retained, since it is a modern and relatively rapidly developing numerical method, yet other, more novel mathematical methods will also be introduced. By using a measuring device which has higher precision, sensitivity and resolution, it will be possible to reconstruct images of higher resolution than those shown here and to detect less obvious or smaller-size anomalies.

Acknowledgement:

This work was supported by grants GINOP-2.3.2.-15- 2016-00022 and EFOP-3.6.2-16-2017-00010.

References:

[1] G. Nicolotti; L.V.Socco; R.Martinis; A. Godio; L. Sambuelli: “Application and comparison ofthree tomographic techniques for detection of decay in trees” *Journal Of Arboriculture*,vol. 29 n. 2, pp. 66-78. 2003.

[2] D. Bieker, S. Rust: “Electric resistivity tomography shows radial variation of electrolytes in Quercus robur”, *Canadian Journal of Forest Research*, 40(6): 1189-1193. 2010.

[3] D. Bieker, S. Rust: “Non-Destructive Estimation of Sapwood and Heartwood Width in Scots Pine (Pinus sylvestris L.)”, *Silva Fennica* 44(2): 267–273., 2010.

[4] D. Bieker, R. Kehr, G. Weber, S. Rust S.: “Non-destructive monitoring of early stages of white rot by Trametes versicolor in Fraxinus excelsior”, *Annals of Forest Science*, Volume 67, Issue 2, pp 210–210. 2010.

[5] N. J.Brazee, R. E. Marra, L. Göcke, P. V. Wassenaer: “Non - destructive assessment of internal decay in three hardwood species of northeastern North America using sonic and electrical impedance tomography“, *Forestry*, Vol. 84, No. 1, 2011.

[6] A. Erkel, A. Meskó, L. Stegena: *Geofizikai Kutatási Módszerek III.*, Felszíni Geofizika, Tankönykiadó Vállalat, Bp. 1970.

[7] F. Divós, K. Csupor, F. Bröker: “Ultrasonic and Stress Wave based Non-destructive Testing of Wood“, *Proc. 8th International Symp. on*

Nondestructive Testing of Wood, Vancouver, WA. 1991, pp 272

[8] F. Divós: “The International Symposium on Non-destructive Testing of Wood“, *Faipar*, 1992/1, pp11-12.

[9] F. Divós, M. Sugiama: “Longitudinal Stress Waves for Detecting the Presence, Location and Size of Defects in Wood and Wood based Composites“ *9th International Symposium on Non-destructive Testing of Wood, Madison*, WI. 1993, pp 218-219.

[10] F. Divós, K. Mészáros: “Root Decay Detection by Stress Wave Technique“, *Proc. pf the First European Symposium on Nondestructive Evaluation of Wood*, p524. Sopron, Hungary, 1994.

[11] L. Gergely, F. Divos: “Possibility of glue-defect detection in solid wood panels with ultrasound“, *Proccedings of the 12th International Symposium on Nondestructive Testing*, Sopron, pp 453. 2000.

[12] I. Standeisky: *Elektrodinamika*; Egyetemi Jegyzet, Széchenyi István Egyetem, Universitas-Győr Kht., Győr, 2007.

[13] D. S. Holder: *ELECTRICAL IMPEDANCE TOMOGRAPHY, Methods, History and Applications*, Institute of Physics Publishing, IOP Publishing Ltd. 2005.

[14] R. Duraiswami, K. Sarkar, G. L. Chahine: “Efficient 2D and 3D electrical impedance tomography using dual reciprocity boundary element techniques“, *Engineering Analysis with Boundary Elements* 22 (PII: S0955-7997(98)00028-9) 13–31, 1998.

[15] M. G. Rasteiro, R. Silva, F. A. P. Garcia and P. Faia: “Electrical Tomography: a review of Configurations and Applications to Particulate Processes“, *Volume 29 Pages 67-80*, 2011.

[16] Description of Tree Inspection Equipment, Argus Electronic Gmbh.

[17] N. Lesparre, A. Adler, D. Gibert, F. Nicollin: “Electrical Impedance Tomography in geophysics“, *Application of EIDORS*, 2011.

[18] K Borbas, T. Kiss, M. Klincsik, Z. Kvasznicza, K. Mathe, Cs. Ver, Z. Vizvari, P. Odry: *Process and measuring system for data acquisition and processing in soft-tomography studies* (in Hungarian) Patent P1500616, 2015.

[19] K Borbas, T. Kiss, M. Klincsik, Z. Kvasznicza, K. Mathe, Cs. Ver, Z. Vizvari, P. Odry: *Process and Measuring System for Data Acquisition and Processing in Soft-Tomography Studies*, US20180374244A1, https://patents.google.com/patent/US20180374244A1/en

[20] Z. Vizvari, T. Kiss, Cs. Ver, M. Klincsik, Z. Sari, K. Mathe, B. Kuljic, F. Henezi, P. Odry: “A multi-channel electrical impedance meter based on digital lock-in technology“; *Pollack Periodica*; (accepted) 2019.

[21] Z. Vizvari, T. Kiss, K. Matha, P. Odry, Cs. Ver, F. Divos: “Multi-Frequency Electrical Impedance Measurement on a Wooden Disc Sample”, *Acta Silvanica et lignaria Hungarica: Forest, wood and environmental sciences* 11:(2) pp. 153-161. 2019.